

Computational Studies of Contact Time Dependence of Adhesive Energy Due to Redistribution of the Locations of Strong Specific Interfacial Interactions

Arlette R. C. Baljon,* Joris Vorselaars, and Travis J. Depuy

Department of Physics, San Diego State University, San Diego, California 92182

Received October 3, 2003; Revised Manuscript Received May 20, 2004

ABSTRACT: The work required to pull a polymeric material from a solid surface with which it connects through hydrogen bonding has been studied by means of molecular dynamics simulations of a coarse-grained bead–spring model. In our simulations, the work, and hence the adhesive energy, increases with the time for which the polymeric material and the surface have been in contact. The work of adhesion G contains a reversible component due to interfacial molecular interactions, as well as an irreversible one, due to dissipative processes. Our data indicate that an increase in the irreversible and not in the reversible work causes G to increase with prolonged contact time. Hence, the phenomenon cannot be attributed to the formation of more or stronger interfacial bonds. Instead, we attribute this increase to a slow redistribution of the beads on the polymer chains that form hydrogen bonds with the surface. Two ways in which this takes effect could be specified. One is that the formation of long loops—chain sections between adjacent bonds—is suppressed after prolonged contact. Another is that over time bonds get distributed more evenly over the polymer backbone and among the polymer chains.

I. Introduction

The work required to pull a polymeric material from a surface naively may be thought to be due to interactions at their interface and hence to equal the increase in surface energy when interfacial bonds break. In reality, it does not work that way at all. Adhesive processes are hysteric and dissipative. The adhesive energy, or work done on separating two surfaces, is larger than the energy released when they come into contact.^{1,2} For instance, no matter how slow the separation takes place, chains close to the interface will stretch before they detach. Upon detachment elastic energy stored in these stretched chains will be dissipated. Dissipative processes may occur in the bulk as well. When a viscoelastic material moves through a series of metastable thermodynamic states, energy dissipation takes place at the transition from one state to the next. Despite many studies of adhesion hysteresis, there is still no complete understanding of this phenomenon and of the relative importance of bulk and surface contributions to the dissipation. In general, it is believed that the adhesive energy of a material can be calculated once the viscoelastic characteristics are known along with the thermodynamic energy.^{1,2} However, not in all cases is it possible to predict the dissipated energy from equilibrium measurements by themselves. The rupture process can be very complex and may need to be understood in its full complexity. This is where computer simulations come in.

Through our current simulations we hope to understand how, in case temporary hydrogen bonds form, adhesive energy is affected by the time a polymeric material and a surface have been in contact, as has been observed in experiments^{3–6} by Ulman et al. In their study a PDMS (polydimethylsiloxane) polymer network and a Si–OH surface are brought into contact, and the

two equilibrate for up to 2 h. It was found that at subsequent rupture the work required to pull the PDMS off the surface increased significantly with contact time. This is believed to be due to structural reorganization of the interface.³ It has been hypothesized that during contact time additional hydrogen bonds form, as the polymer relaxes near the interface, or that existing ones grow stronger as Si–OH and siloxane groups in the PDMS align. More or stronger hydrogen bonds will cause the energy dissipated upon their detachment to increase. This might account for the observed increase of adhesive energy with contact time. It is conceivable, though, that the increase in adhesive energy does not result from the formation of more or stronger hydrogen bonds but that internal rearrangement takes place in which hydrogen bonds form at new locations along the polymer backbone, while old ones release. This new hydrogen bond configuration may be such that it takes more work to separate the polymer and surface. For instance, rupture involves not only the breaking of original hydrogen bonds but also the formation of new ones that subsequently must be broken. Minor variations in the location of polymer beads that connect to the lower silicate surface may cause a noticeable increase in the total number of hydrogen bonds that must be broken.

The goal of this study is to explore the reason for the contact time dependence of adhesive energy. In our simulations, we use a simplified model in which a polymer brush adheres to a surface by a combination of Lennard-Jones (LJ) interactions and thermal activated temporary bonds. Although in experiments both bulk and surface effects contribute to energy dissipation, the contact time dependence of the adhesive energy appears to be mainly due to the surface effects.⁴ When no specific bonding between the polymer and the surface occurs, adhesive energy is independent of contact time.^{3,6} On the other hand, when hydrogen bonds are replaced by stronger deuterium ones, the adhesive hysteresis as

* To whom correspondence should be addressed. E-mail: abaljon@mail.sdsu.edu.

well as its dependence on contact time increases.^{4,6} Hence, we believe that our simplified model captures those features necessary to study how the formation of specific bonds between the polymer and surface gives rise to contact time dependence of adhesive energy. In particular, we expect that our conclusion that the increase in adhesive energy is not due to the formation of more and stronger bonds, but instead caused by a change in the architecture—that is the location of hydrogen bonds—is valid for more complex systems as well.

Several groups have studied the adhesive strength of materials through simulations.^{7–11} In most of their studies, the polymeric material is cooled below the glass transition temperature and subsequently ruptured. In the study at hand the temperature is kept slightly above that of the glass transition, since slow relaxation and aging phenomena typically occur in this temperature range. The viscoelastic response to strain in both cases is quite different. While glassy materials yield at a critical strain and subsequently form crazes,^{8,11} in the current simulations a smooth decrease of the stress with increased strain is observed.

Slow relaxation of polymers near interfaces has been studied extensively, for instance in experiments using the surface forces apparatus.^{12,13} In particular, we will compare our results to those obtained in a study by Raviv et al.¹⁴ of extremely slow relaxation of a viscoelastic polymer layer near a strongly attractive surface. Layers of bound polymers occur in nanocomposite materials where strongly attractive inorganic particles are interspersed in a polymer matrix. The mechanical properties of these new composites are puzzling, especially in the nonlinear regime, where “memory” of previous deformations appears to be preserved for hours.¹⁵ Most likely the relaxation characteristics of the so-called “bound” polymer layer close to the nanoparticles play a role in these phenomena. Similar questions come up in studies of cell adhesion and tissue engineering, in which case temporary bonds or binders are caused by ligand/receptor^{16–18} pairs. Also in this case investigators would like to understand if slow changes in properties and function of the biological systems are caused by an increase in the strength of the individual ligand/receptor bonds or by a change in global organization, dictated by, among other things, the location of ligand/receptor bonds.¹⁸

II. Simulation Method and Model

In our molecular dynamics simulations 32 polymer chains are modeled as a bead–spring necklace.¹⁹ Each of the 32 polymers is 128 beads long. The model has been successfully employed in previous adhesion studies.^{7–11} Each bead represents several atoms. Beads interact through a truncated and shifted Lennard-Jones (LJ) potential²⁰

$$V_{\text{LJ}}(r) = 4\epsilon[(\sigma/r)^{12} - (\sigma/r)^6 - (\sigma/r_c)^{12} + (\sigma/r_c)^6] \quad \text{if } r \leq r_c \quad (1)$$

and zero otherwise. Its energy scale ϵ , length scale σ , and time scale $\tau = \sigma(m/\epsilon)^{1/2}$ define the units in which all the calculated quantities are expressed. The cutoff range $r_c = 2.2\sigma$. The algorithm is implemented using a fifth-order Gear predictor–corrector algorithm with $\Delta t = 0.005\tau$.

In addition, a strong anharmonic spring potential (FENE)¹⁸ connects beads in the chain structure:

$$V_{\text{FENE}} = -\frac{1}{2}\kappa R_0^2 \ln[1 - (r/R_0)^2] \quad (2)$$

where $R_0 = 1.5\sigma$ and $k = 30\epsilon/\sigma^2$. The parameters κ and R_0 are set such that the chains cannot cross. The silicate surface is modeled as two planes of a (111) face-centered-cubic lattice with nearest-neighbor distance 1.2σ . The surface atoms do not interact with each other. Each atom is bound to its lattice site by a stiff harmonic spring with spring constant $\kappa = 260\epsilon/\sigma^2$. It is adjusted so that thermal displacements are small compared to the Lindeman criterion of melting.²¹ Lattice atoms and polymer beads interact through the same LJ potential; in this case a different cutoff range $r_c = 2^{1/6}$ is employed. A Langevin thermostat¹⁹ with damping constant $4\tau^{-1}$ is used to control the temperature. The heat bath is coupled only to the surface atoms, which mimics the experimental situation. Although during rupture the interior of the polymer film heats slightly, this is never more than a few percent. The simulations are performed at a temperature $T = 0.6\epsilon/k_B$, at which the polymer deforms viscoelastically. Changes in temperature affect the state of the polymer. The glass transition temperature (T_g) of this model has been estimated at $(0.4 - 0.5)\epsilon/k_B$.⁸ A detailed study of T_g and its dependence on the strength of the interaction between surface atoms and polymer beads will be published in a forthcoming paper.²² What is most important for this work is that the response of the system to stress, as we will show below, is the one typical for a viscoelastic system at a temperature above T_g .

Temporary bonds are modeled by the FENE potential. Each atom on the surface can only form one bond with a bead on a polymer. Once every 20 time steps it is attempted to create and destroy temporary bonds. This is a Monte Carlo step in which the creation or destruction of a bond is accepted with a probability calculated from the energy difference between the new and old states. The energy is the sum of the FENE potential and a (negative) constant U_{assoc} , which represents the associative chemical interaction through which the bonds are formed. Because of the stiffness of the FENE potential, attempts to break stretched temporary bonds often succeed. In this study we set $U_{\text{assoc}} = -22\epsilon$. If the value of U_{assoc} is decreased below -23ϵ , the polymer wets the surface.

Figure 1 outlines the simulation model. The simulation cell contains two solid surfaces: the lower silicate one and the upper grafting one. The grafting surface is modeled like a silicate surface, except that at the former no temporary bonds with polymers form. Instead, an end bead of each polymer is permanently attached to one of its atoms with a FENE potential. The location of the grafting sides is randomly chosen inside a circle with radius 12σ . The system is equilibrated for 30000τ , at which point statistical quantities, such as the radius of gyration, fluctuate around their average values. The number density in the initial state is approximately $1\sigma^{-3}$. At this density the entanglement length N_e is approximately 50.⁸ Hence, the chains are slightly entangled. In the initial state after equilibration the average radius of gyration (R_g) of the chain molecules in the direction parallel to the surface is within 5% of the R_g perpendicular to it (z -direction). Hence, the grafting density is such that the polymers are halfway

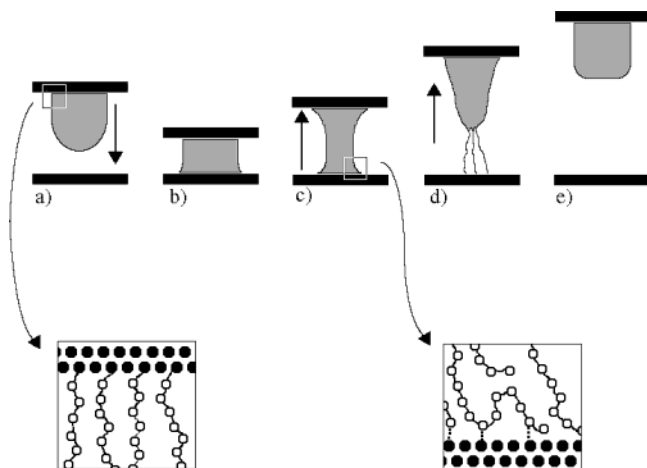


Figure 1. Simulation model. The black bars model the grafting and silicate surfaces and the gray areas the polymer melt. Situations (a) to (e) occur progressively in time. Arrows indicate the motion of the top surface. The blow-ups show the fcc lattices (closed circles) and polymer beads (open circles). Permanent bonds are shown by solid lines and temporary ones by dotted lines.

between the so-called “brush” and “mushroom” regimes. Note that we do not employ periodic boundary conditions.

Subsequently, (a) the surface on which the polymers are grafted is slowly lowered at $v = 0.1\sigma/\tau$. The polymers start to make contact with the silicate surface, which is parallel to the grafting surface. The motion stops when the separation of both surfaces equals 12σ . This results in a polymer melt of approximately cylindrical shape. The simulation is continued (b) at a fixed plate separation. We allow the system to equilibrate for up to 60000τ , during which time period temporary bonds between polymer and lower surface continuously form and break. At several stages of the equilibration process the polymer and the silicate surface are separated. To this end the grafting surface is moved outward with a speed $v = 0.1\sigma/\tau$ (c). Since the polymers are attached to this surface, they will have to move with it. Chains stretch and bond lengths slightly increase (d). During none of our runs bond lengths reach the critical value necessary to rupture them.⁸ Instead, the system fails by breaking the stretched temporary bonds. Finally, (e) the temporary bonds between the polymer and lower surface break.

Complete rupture is attained after a time of approximately 700τ . The force required for rupture is calculated from the interactions between the grafting surface and polymer melt. An integral of this force over the displacement of the top wall yields the total work required for each rupture process, also called the adhesive energy G .

III. Results and Discussion

Figure 2 shows the work as a function of displacement for three different contact times: 27500τ , 45000τ , and 60000τ . The data saturate at a constant value, reached after completion of rupture. This value is the adhesive energy G . Each curve is obtained from an average of two rupture runs separated by a time interval of 150τ . One observes an overall increase in the work with longer contact time. Hence, our simple brush polymer model yields results that are qualitatively similar to the more complex experimental systems. Table 1 shows data for

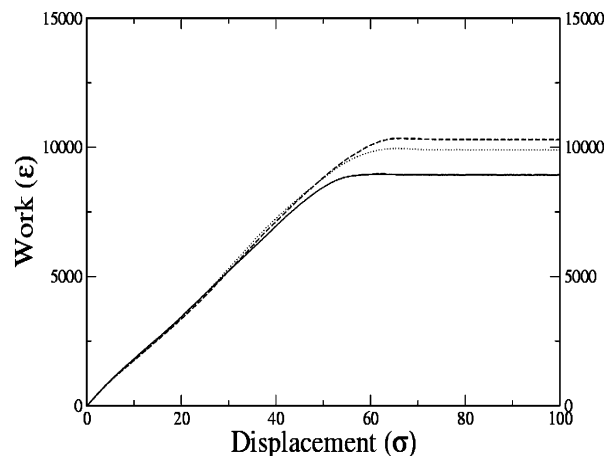


Figure 2. Dependence of the adhesive energy G on the time that the polymer and bottom surface have been in contact. Data are shown for three contact times: 27500τ (solid), 45000τ (dotted), and 60000τ (long dashed).

the same three contact times. Columns 1 and 2 give the contact time and adhesive energy G , and column 3 gives the total number of bonds before rupture starts. Although the number of bonds increases slightly, this effect cannot explain the increase in G . As can be seen in column 4, the adhesive energy per bond increases as well. In the process of rupture, bonds are continuously formed and broken. Column 5 gives the total number of temporary bonds broken in each separation. This includes those present before and those formed in the rupture process. Column 6 gives the work/bond for this case. Comparing the data at each contact shows that, if a certain amount of work is tentatively associated with each bond, the number of bonds broken in the process is a slightly more accurate measure for the total work required than the number of bonds before rupture starts. We will show that the increase in the number of bonds that need to be broken results from a longer rupture path. This in turn is caused by a change in the distribution of temporary bonds on the polymer chains. One would expect the adhesive energy to vary with the time interval between efforts to create or destroy temporary bonds. Table 1 shows values for an attempt every 0.1τ . These data are, in Table 2, compared with those obtained for less and more frequent attempts. It can be concluded that the adhesive energy indeed depends on the attempt frequency. A roughly similar increase in adhesive energy, however, occurs with prolonged contact time. In experimental systems this characteristic time can be increased by replacing hydrogen by deuterium. Ulman et al.⁴ found that this indeed increases the adhesive energy. The increase in turn increases with prolonged contact time. This perfectly matches our computational results. In Table 2, the increase from the first to the last column equals 1890ϵ at 27500τ and 1966ϵ at 60000τ . Ulman et al. have argued⁴ that this contact time dependence may be due to rearrangements of the polymer conformation near the surface. Our computational studies confirm this hypothesis. We shall recur to this momentarily.

Figure 3a shows the force and Figure 3b the number of temporary bonds during rupture for two contact times. The number of bonds and the force are initially similar for both contact times. However, after the two plates have been displaced over a distance of 20σ or more, there is a difference. The longer the contact time, the higher the force and the number of temporary bonds

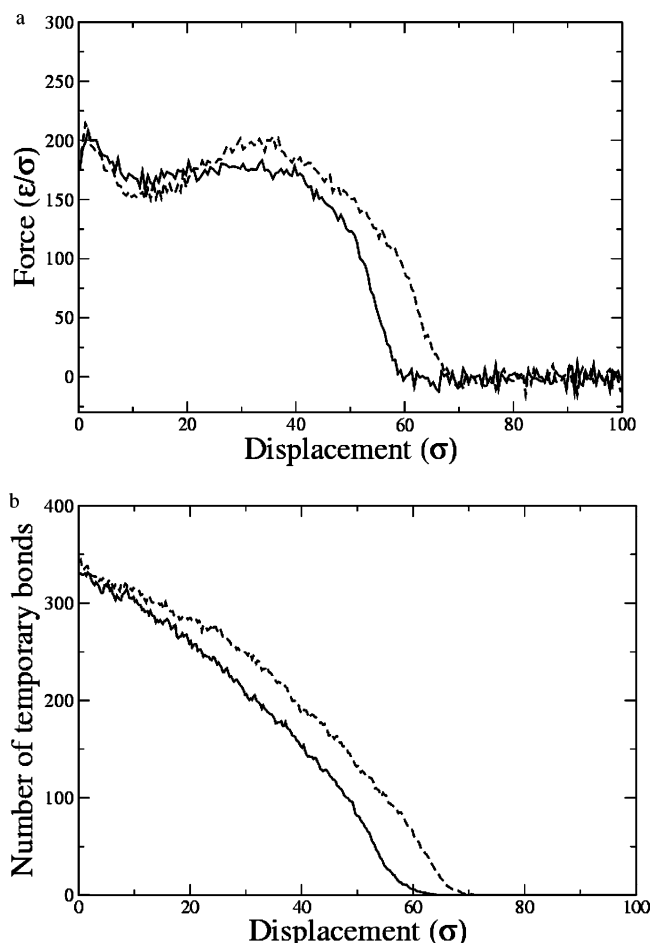
Table 1. Data for Rupture Runs; See Text for Details

contact time (τ)	$G(\epsilon)$	no. of bonds before rupture starts	work/no. of initial bonds (ϵ)	no. of bonds broken during rupture	work/no. of broken bonds (ϵ)
27500	8928 ± 180	327	27.8	11 672	0.78
45000	9901 ± 130	336	29.5	12 511	0.79
60000	10290 ± 195	342	30.3	14 009	0.74

Table 2. Dependence of the Adhesive Energy G on the Frequency at Which Attempts Are Made To Form and Break Temporary Bonds^a

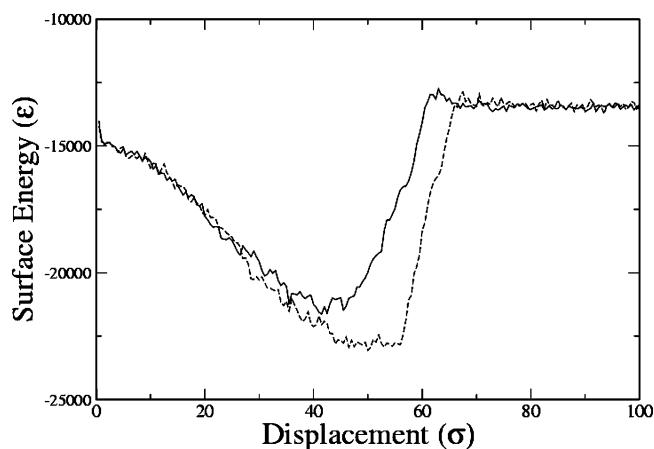
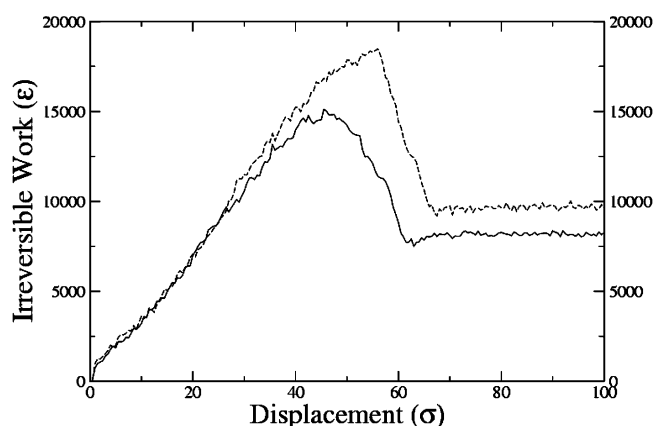
contact time (τ)	G (attempt rate 0.05τ)	G (attempt rate 0.1τ)	G (attempt rate 0.2τ)
27500	8190 ± 130	8928 ± 180	10080 ± 209
60000	9410 ± 20	10290 ± 195	11376 ± 198

^a Note that, as expected, the absolute value of G depends on the attempt rate. In all three cases, though, G increases with prolonged contact time.

**Figure 3.** Force (a) and total number of bonds left (b) during rupture. Data are shown for two contact times: 27500 τ (solid) and 60000 τ (long dashed).

that remain connected. What this suggests is that the observed contact time dependence is not due to the formation of more and stronger bonds. When this would have been the case, the force and number of temporary bonds would have been higher after longer contact for small displacements as well.

The same can be concluded from a calculation of the reversible part of the work. Figures 4 and 5 show for the same two contact times the contributions of the reversible surface energy and irreversible dissipative energy separately. To this end, the surface tension has been calculated from the difference between the normal and tangential components of the pressure–stress ten-

**Figure 4.** Reversible surface energy as a function of displacement of top surface. Data are shown for two contact times: 27500 τ (solid) and 60000 τ (long dashed).**Figure 5.** Irreversible dissipative energy as a function of displacement of top surface. Data are shown for two contact times: 27500 τ (solid) and 60000 τ (long dashed).

sor using the Kirkwood–Bluff formulation.^{20,21,23} The surface energy is obtained from an integral of the surface tension over the xy plane. The reversible work equals the change in surface energy over the length of the rupture process. It equals 666 ϵ for a contact time of 27500 τ and 685 ϵ for 60000 τ . This small increase (3%) corresponds to a small increase (2%) in the number of temporary bonds in the states before rupture (see Table 1). This increase is negligible compared to that in the dissipated energy, shown in Figure 5. This total energy dissipated increases from 8262 ϵ to 9605 ϵ or by 16%. This large increase cannot be due to the formation of a few more bonds. It must be contributed to a different rupture route, in which temporary bonds are broken more gradually. Please note the peak in the dissipated energy, indicating that whereas heat initially flows into the system, the process is reversed after the last temporary bond breaks. At that time the surface of the polymer brush is extremely distorted. When it relaxes back to its equilibrium shape, surface energy decreases and heat flows toward the heat bath.

Before investigating the bond distribution in more detail, let us see what the effect is of decreasing the

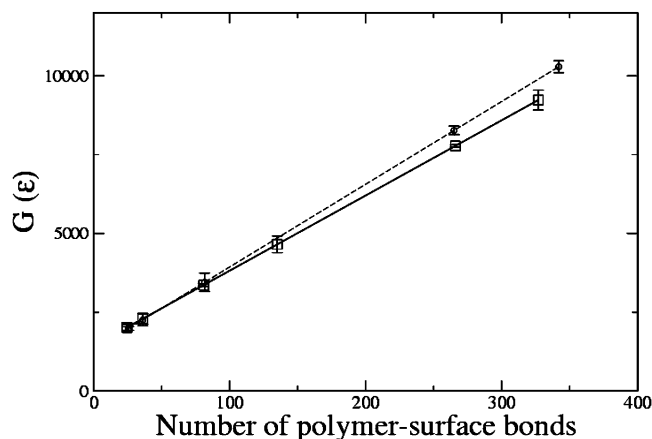


Figure 6. Adhesive energy G as a function of number of temporary bonds. The number of temporary bonds varies due to the variation of the fraction of beads in the lower surface, which are allowed to bind with the polymers. Data are shown for contact times of 27500τ (square) and 60000τ (circle). All data points and error bars are obtained from averages over two rupture runs. Both data sets can be fitted with a line.

number of bonds. To do so we vary the concentration of lattice sites that can form temporary bonds, the so-called active sites. At the onset, all atoms of the surface can form bonds. This concentration is lowered, while keeping the distribution uniform. The value of U_{assoc} stays fixed at -22ϵ . Several experimental groups^{5,24} have done the same and found that the adhesive energy depends on the number of active sites and hence on the number of temporary bonds that will actually form.

Figure 6 reveals that in our simulations the adhesive energy increases linearly with the number of temporary bonds that form. Data are shown for the same two contact times, 27500τ and 60000τ . If just a few bonds are present, the contact time dependence appears to be negligible. This is in agreement with experimental observations³ which indicate that the contact time dependence is due to the hydrogen bonds and disappears when only noncovalent bonds are involved. For both contact times the data points can be fitted by a linear curve. Its slope is steeper after longer contact time. This is not due to wetting since the number of bonds and the size of the surface area in which they form are more or less independent of contact time. Naively one might think that each temporary bond grows stronger over time, but no such a mechanism has been accounted for in the simulations model. Nor did we find that the density of the polymer film near the bottom wall increases with prolonged contact time. Hence, an alternative description of a “bond”, based on the collective binding of several beads nearby on the chain structure, is needed. Such collective binding can be observed in snapshots of the configurations during the rupture process, such as those shown in Figure 7.

In what follows, a cluster of bonds is defined as being formed by at least two beads that are less than four separated on the chain structure. Figure 8 shows the number of clusters before rupture vs cluster size for both contact times. It turns out that during prolonged contact the largest clusters tend to break up, while intermediate ones with 6–12 contacts form. At a contact time of 60000τ , the total number of clusters before rupture is slightly higher than at 27500τ (63.14 instead of 57.86).

One wonders if this might be what causes the increase in force. Does it take more work to rupture many small clusters than a few large ones? To address this question,

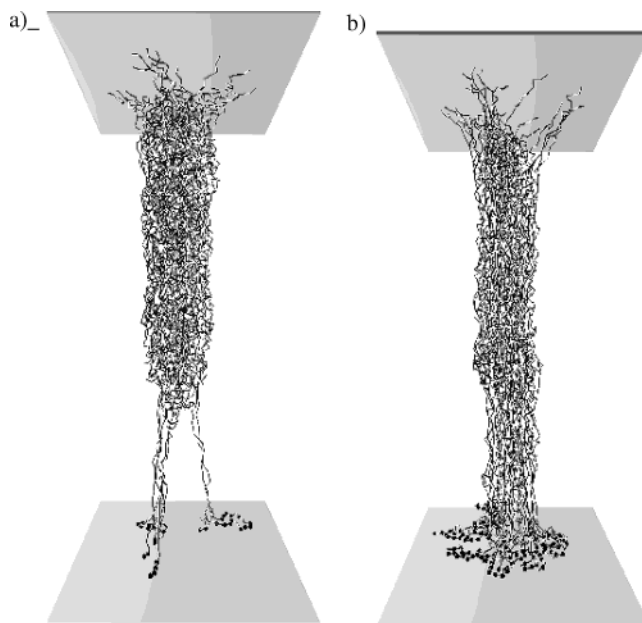


Figure 7. Snapshots of the rupture process after a displacement of the top wall by 55σ . In (a) the contact time is 27500τ and in (b) 60000τ . Beads on polymers that bind with the bottom surface are shown as spheres.

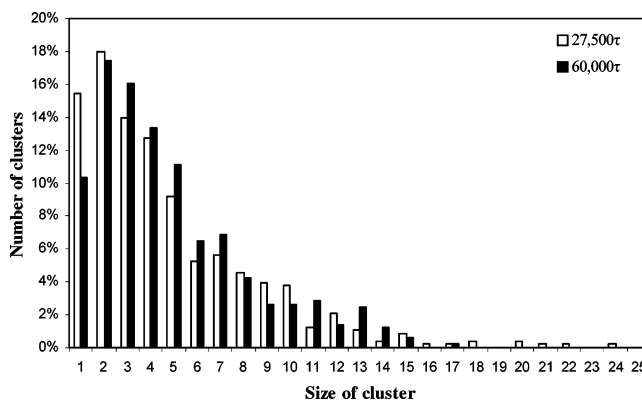


Figure 8. Distribution of cluster sizes before rupture for the same two different contact times.

the lifetime of clusters as a function of cluster size was measured. A cluster is allowed to fluctuate in size or slightly change its position. It ultimately “dies” when the last bond ruptures from the surface. Figure 9 shows the results. Instead of the time, the distance over which the upper surface has moved is shown. Large clusters (> 7) live longer after increased contact time. Moreover, lifetime increases strongly with cluster size of up to nine bonds. After that it is relatively independent. Hence, we conclude that when cluster size exceeds nine bonds, breaking it up into smaller ones will result in a configuration that requires more work to rupture. Each of the individual clusters has to be broken off separately.

An alternative way to characterize which beads on polymers bind with the surface is to study the distribution of loop lengths between two successive contacts of a polymer chain. This measure is given in Figure 10. The probability P for a loop to have a length n scales as

$$P(n) \approx n^{-\alpha} \quad (3)$$

where $\alpha = 1.6 \pm 0.1$ for low n . This distribution has been analytically obtained in the literature.²⁵ Polymers in a dense melt obey the statistics of Gaussian random

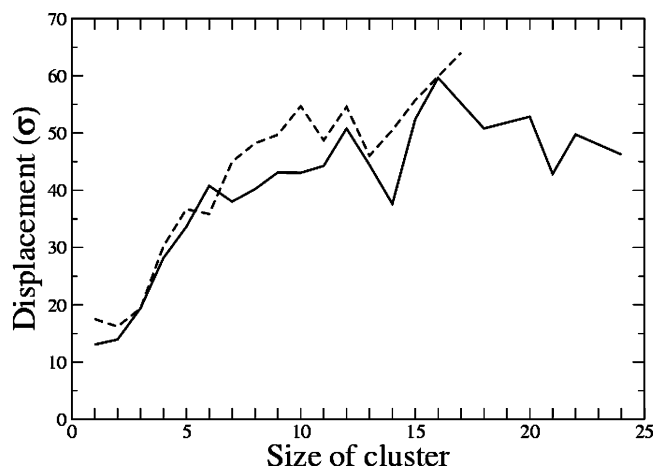


Figure 9. Lifetime of a cluster. For a cluster of certain size it has been measured how far the walls have been separated before the last bond in the cluster breaks. Data are shown for contact times of 27500τ (solid line) and 60000τ (dashed line).

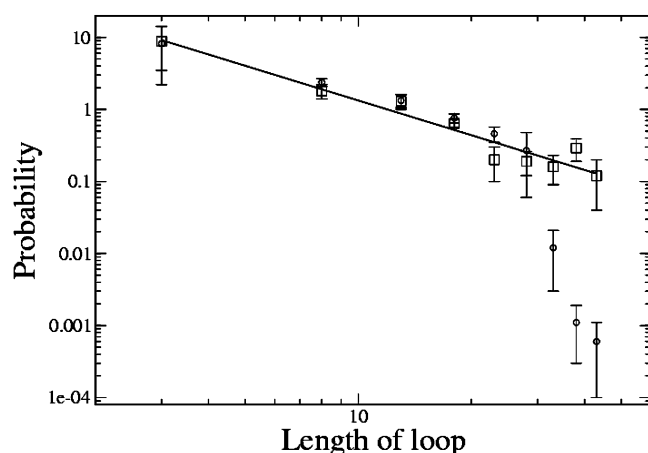


Figure 10. Probability to find a loop—chain segment between two temporary bonds—of certain length. Data are plotted logarithmic and fitted by a line with a slope $\alpha = 1.6 \pm 0.1$. Data are shown for contact times of 27500τ (squares) and 60000τ (circles). The longest loops disappear after prolonged contact.

walks. Hence, the distribution of lengths between successive contacts with a wall is given by formula 3 with $\alpha = 1.5$. Our data follow this law for small loop sizes. Of particular interest is the deviation from this scaling behavior for long loops ($n > 25$) after prolonged contact. We attribute this to the presence of the grafting wall. Loops with $n > 25$ will extend all the way to the grafting wall, which distorts their conformation. As Raviv et al.¹⁴ have calculated, the probability to find the longer loop is suppressed; power law falloff is replaced by exponential falloff. This relaxation process is slow due to the nonlocal nature of the process. Re-formation of temporary bonds near the bottom surface changes the conformation of polymers near the top surface. An increase in adhesive energy due to the absence of the longest loops can be understood as follows. When they exist, they exert a repulsive normal force on the top surface. The existence of this normal force lowers the work required for rupture. For clarity, Figure 10 gives data for two contact times. We found that, for an intermediate contact time (45000τ), loops are suppressed as well, although to a lower extent as for the longest contact time (60000τ).

Table 3. Characteristics of the Configuration at Three Different Contact Times^a

contact time (τ)	av bonds per polymer	variation	no. of polymers with bonds
27500	10.4	10.5	25
60000	10.8	10.2	26

^a All values are obtained from averages over a period of 300τ .

Finally, we investigated the distribution of bonded beads over the 32 chains. Table 3 shows the results for two contact times. All data are averaged over a period of 300τ . The average number of bonds on each of the 32 polymers is around 10.5, but with a wide variation. Some polymers contain up to 50 bonds and others none at all.

A small drop in the variation as a function of contact time can be observed. This is consistent with the disappearance of the longest loops. A better distribution of the bonds over the chains is another cause of the increase in adhesive energy over time.

IV. Conclusions

Our simulations reveal that the adhesive energy of a viscoelastic polymeric brush in contact with a solid surface with which it connects through hydrogen bonding increases with the time a polymer and surface have been in contact. Comparing the data for two contact times in detail, we see that the increase in reversible surface energy is less than 3%, while the overall increase in adhesive energy is more than 15%. Hence, the common notion^{1,26} that the adhesive energy is proportional to the reversible work does not appear to hold in the presence of temporary bonds between a polymer and surface. Instead, molecular level investigations reveal that minor variations in the location of beads on the polymer chain structure that connect to the lower silicate surface during contact time cause an increase in dissipation but not in surface energy. Two mechanisms in particular have been shown to be at work:

1. The number of clusters of bonded beads increases with prolonged contact. At the same time, the average number of bonds per cluster decreases. When the polymer melt first contacts the lower silicate surface, large clusters of bonds form on the first chain sections that reach the surface. During contact these large clusters slowly break up and more, intermediate ones form. Bonded beads distribute themselves more evenly over the various chains. Both changes are minor yet tend to increase the adhesive energy. Other changes in the states before rupture may occur that we have not discovered yet.

2. The formation of long loops—chain sections between adjacent bonds—is suppressed after prolonged contact. Since the longest loops exert a repulsive force on the grafting wall, this will cause an increase in adhesive energy.

To estimate the relative contribution of each of these effects, we investigated the force exerted by the polymer on the grafting wall in more detail. The adhesive energy is obtained from the integral of this force over distance. The first of the above mechanisms will cause a change in the forces (FENE and LJ) between the grafted beads and the wall and the second a change in the LJ forces between the atoms in the wall and other beads on the polymers. These forces have been calculated separately, and it turns out that approximately 20% of the total

work is due to forces caused by interactions between surface and unbound beads, while the rest is due to interactions with the grafted beads. Increasing contact time from 27500τ to 60000τ , the total work increases with 15%. This is due to a 12% increase in the work required to pull on the chains connected to the grafted beads, while the contribution of the unbound forces to the work increases by 27%. Hence, both mechanisms contribute.

Even though in this study temporary bonds are modeled at a mesoscopic level, important conclusions can be made. For the future, it might be interesting to do similar studies with atomistic level simulations. Interactions and equilibrium structures of PDMS at silicon dioxide surfaces have been recently studied by Tsige et al.²⁷

The slow kinetics of a polymer in contact with a strongly attractive surface, as here observed, is consistent with studies by Raviv et al.¹⁴ These authors are interested in the recovery of equilibrium structure during rebound of a confined polymeric film. Full relaxation takes minutes to hours and is most likely caused by a slow redistribution of binding sites. In particular, it is due to the formation of long loops, which did not occur in the confined state.

Slow kinetics occur in biological system as well, in particular in the mechanical attachment of a cell through specific ligand/receptor interactions.^{16,17} Although the specifics of the thermodynamic forces in cases at hand vary widely, the physical origin of the slow kinetics could be due to a common phenomenon: a very slow change in location and distribution of the specific binding sites.

Acknowledgment. This research is supported by an award from Research Corporation. Moreover, Joris Vorselaars has contributed to this work during a 3 month long student internship. He acknowledges support from the Department of Applied Physics of the Technical University Eindhoven, The Netherlands.

References and Notes

- (1) Maugis, D. In *Adhesion and Friction*; Gunze, M., Kreuzer, H., Eds.; Springer-Verlag: Berlin, 1990.
- (2) Pocius, A. V. *Adhesion and Adhesive Technology: An Introduction*; Hanser: Munich, 1997.
- (3) Kim, S.; Choi, G. Y.; Ulman, A.; Fleischer, C. *Langmuir* **1997**, *13*, 6850.
- (4) Choi, G. J.; Ulman, A.; Shnidman, Y.; Zurawsky, W. J.; Fleischer, C. *J. Phys. Chem. B* **2000**, *104*, 5768.
- (5) Choi, G. Y.; Zurawsky, W.; Ulman, A. *Langmuir* **1999**, *15*, 8447.
- (6) Ulman, A.; Choi, G.; Shnidman, Y.; Zurawsky, W. *Isr. J. Chem.* **2000**, *40*, 107.
- (7) Baljon, A. R. C.; Robbins, M. O. *Science* **1996**, *271*, 482.
- (8) Baljon, A. R. C.; Robbins, M. O. *Macromolecules* **2001**, *34*, 4200.
- (9) Stevens, M. J. *Macromolecules* **2001**, *34*, 2710.
- (10) Gersappe, D.; Robbins, M. O. *Europhys. Lett.* **1999**, *48*, 150.
- (11) Rottler, J.; Robbins, M. O. *Phys. Rev. E* **2003**, *68*, 011801.
- (12) Drummond, C.; Israelachvili, J. *Macromolecules* **2000**, *33*, 4910.
- (13) Eframova, N. V.; Huang, Y.; Peppas, N. A.; Leckband, D. E. *Langmuir* **2002**, *18*, 836.
- (14) Raviv, U.; Klein, J.; Witten, T. A. *Eur. Phys. J. E* **2002**, *9*, 405.
- (15) Sternstein, S. S.; Zhu, A. *Macromolecules* **2002**, *35*, 7262.
- (16) Bruinsma, R.; Sackmann, E. *C. R. Acad. Sci. Paris, t.2, Ser. IV* **2001**, 803.
- (17) Brochard-Wyart, F.; DeGennes, P. G. *Proc. Natl. Acad. Sci.* **2002**, *99*, 7854.
- (18) Lauffenburger, D. A.; Griffith, L. G. *Proc. Natl. Acad. Sci.* **2001**, *98*, 4282.
- (19) Kremer, K.; Grest, G. *J. Chem. Phys.* **1990**, *92*, 5057.
- (20) Allen, M. P.; Tildesley, D. J. *Computer Simulations of Liquids*; Clarendon: Oxford, 1987.
- (21) Thompson, P. A.; Robbins, M. O. *Phys. Rev. A* **1990**, *41*, 6830.
- (22) Baljon, A. R. C.; Van Weert, M. H. M.; Barber-DeGraaff, R.; Khare, R., manuscript in preparation.
- (23) Kirkwood, J. G.; Bluff, F. P. *J. Chem. Phys.* **1949**, *19*, 539.
- (24) Kent, M. S.; Yim, H.; Matheson, A.; Cogdill, C.; Nelson, G.; Reedy, E. D. *J. Adhes.* **2001**, *75*, 267.
- (25) Guiselin, O. *Europhys. Lett.* **1992**, *17*, 225.
- (26) Gent, A. N.; Lai, S. M. *J. Polym. Sci., Part B* **1994**, *32*, 1543.
- (27) Tsige, M.; Soddemann, T.; Rempe, S. B.; Grest, G. S.; Kress, J. D.; Robbins, M. O.; Sides, S. W.; Stevens, M. J.; Webb, E. *J. Chem. Phys.* **2003**, *118*, 5132.

MA035492P